This is the author's version (accepted manuscript) of the work that was accepted for publication in IEEE Transactions on Smart Grid.
The Version of Record is available online at https://doi.org/10.1109/TSG.2023.3280326

Load Recognition in Hardware-Based Low Voltage Distribution Grids using Convolutional Neural Networks

Henning Schlachter, Stefan Geißendörfer, Karsten von Maydell, Carsten Agert

***Abstract*—Due to climate targets of the German government, the share of renewable energy in the power grid will be increased and the number of grid participants connected to the low voltage level of the power grid will rise. This leads to new requirements in voltage control, especially in low voltage distribution grids. In order to achieve a stable power grid in future, further development of control strategies is necessary. In this paper, a load recognition concept, which was tested on simulative data in previous work, is further developed to reduce simulation effort. Additionally, the concept is adapted for real hardware influences and active grid participants complicating the recognition task. Thus, the main contribution of this study is the successful application of the methodology within a hardware-based test grid containing a charging electric vehicle. Using a convolutional neural network in a time series classification setting, the recognition rates in this use-case exceeded 99 % while benefiting from an asymmetric charging behavior. Due to these promising results, future voltage control strategies could be supported based on gained information through integration of the presented concept.**

***Index Terms*—convolutional neural networks, deep learning, electric vehicles, load recognition, low voltage distribution grids, grid management.**

I. Introduction and Motivation

DUE to the climate targets from national and international agreements, the German power grid is changing in terms of generation and consumption [1]. The German government plans to increase the share of renewable energy in the power grid to $65\,\%$ in 2030 [2], which leads to a decentralized power grid architecture with fluctuating feed-in [3]. In addition, the expansion of e-mobility and the increasing use of electrical heat pumps are being pushed forward [1], [4]. Both technologies are examples to illustrate the increasing number of grid participants, especially in low voltage distribution grids. Fluctuations in feed-in, the number and types of active loads affecting the grid voltage, as well as flexible properties like mobility in the grid, e. g., of electric vehicles (EVs), cause new requirements for reliable power grid operation [3], [5], [6]. Especially the local differences in the power grid and the rapidly changing grid situations mean that the voltage control at different grid connection points of the power grid has to overcome very different challenges and there is a need for adjustments in voltage stabilization to keep the voltage in the tolerance band of $\pm 10\,\%$ of the nominal voltage [3], [7]. Therefore, the field of voltage control is a highly relevant research area, e. g., investigating new methods based on reinforcement learning [8]–[10].

H. Schlachter, S. Geißendörfer, and K. von Maydell are with the Energy Systems Technology Department, Institute of Networked Energy Systems, German Aerospace Center (DLR), Oldenburg, Germany (H.Schlachter@dlr.de, Stefan.Geissendoerfer@dlr.de, Karsten.Maydell@dlr.de). C. Agert is head of the Institute of Networked Energy Systems, German Aerospace Center (DLR), Oldenburg, Germany (Carsten.Agert@dlr.de).

Manuscript received November 23, 2022; revised March 16, 2023; accepted May 14, 2023.

A. Related Work

Another approach contributing to more efficient energy consumption and a stable grid is the concept of non-intrusive load monitoring (NILM) dealing with disaggregation of load profiles from households, founded by Hart [11]. A review of different strategies in this field was given in [12]. Next to this, many more specified contributions were published, e. g., presenting NILM approaches based on unsupervised learning and recurrent neural networks [13], [14]. In addition, unsupervised and supervised approaches were compared before developing an unsupervised learning technique for household profile disaggregation in [15]. In context of EVs, a NILM-based method to extract load patterns of charging EVs was developed in [16]. Furthermore, machine learning algorithms were used in a temporal multi-label classification setting including a sliding window approach, which is comparable to this study [17].

The approaches of NILM often are based on data acquired directly at a building's grid connection point and are designed to observe the events in that building. Instead of investigating only connected loads in a household, this study deals with a concept to detect particular loads in the surrounding local grid which strongly affect the grid voltage.

For this approach, the simulative proof of concept based on recognition of electric vehicles was given in previous work of the authors in [18], which did not cover disturbances of unknown loads. Therefore, the next step was to investigate the recognition capability under influences of households still using simulative data in [19].

Since an algorithm applied in real power grids has to deal with far more complex conditions to recognize loads due to hardware properties, measurement inaccuracies, and power grid typical noise, a hardware-based validation of the concept is required. For this purpose, it is necessary to combine simulation models and real hardware devices. This

is generally possible within the hardware-in-the-loop (HIL) framework. For example, this framework was applied to develop an internet-of-things HIL architecture for investigations of frequency regulation by demand response to overcome missing real-world data in [20]. In addition, HIL was used to check speed control design for EVs in [21], while the real-time feasibility of a reinforcement learning energy management strategy for hybrid electric tracked vehicles was tested in [22]. Furthermore, a test on maximum power point tracking of photovoltaic systems using a support vector machine approach in HIL environment was performed in [23]. In total, there are many applications of HIL in various topics.

The concept of power hardware-in-the-loop (PHIL) is very related to HIL and is more relevant to the context of power grid simulations. For example, PHIL framework was used to study the impact of EVs charging on low voltage distribution grids in [24]. Moreover, inverter features such as voltage regulation and frequency response were examined in PHIL environment [25]. Next to this, the response behavior of real power components within a PHIL based grid simulation environment in real-time was investigated [26]. Additionally, two PHIL approaches for testing of smart grid controls were compared in [27].

B. Contribution and Paper Organization

Similar to the NILM concept, an approach of load recognition based only on the measured voltage at a single grid connection point in a real low voltage distribution grid is applied in this study. The used method deals with the investigation of the grid voltage to identify trained loads, especially from surrounding grid connection points, using a convolutional neural network.

For the proposed study, an approach for power grid simulation within PHIL framework, shown in [28], is fundamental. In detail, they used the concept to combine a simulation model of one part of a power grid and a part of the same grid which is realized in hardware.

Following this idea for the investigation in this paper, a low voltage grid is implemented in hardware.

Thus, in the proposed study, a hardware-based test environment for a machine learning approach is implemented, in which the real charging behavior of an EV is emulated, to finally apply the developed methodology for load recognition using a CNN.

By this, the main contributions of this study are as follows:

- In this work, the proposed concept of load recognition is successfully applied in real hardware environment emulating a realistic low voltage distribution grid. By training with the developed methodology, a CNN is enabled to recognize a target load class in the voltage signal despite typical power hardware effects and disturbances of realistic grid participants.
- In the proposed method of training data generation, the simulative generation of voltage profiles is replaced by an inversion of the typical power profile of the component which should be recognized. Thus, simulation effort is reduced.
- For demonstration, a simple test environment is set up, in which a CNN is required to recognize the charging process of a real EV. The CNN is tested in several scenarios at different grid connection points to finally prove the ability to detect the particular EV showing an asymmetric charging behavior. This use-case covers for the first time an asymmetric load using the proposed methodology. It shows the advantage of using voltage from three phases and illustrates the ability to use historical pattern as well as the relation of the phases without calculating phase angles for time series classification. Hence, a real occurring load is detected under real hardware conditions as they are also present in the real power grid.

This paper is organized as follows. In Section II, the overall concept to recognize loads in low voltage grids is explained and its implementation in a real hardware environment is described. Subsequently, Section III deals with the results obtained from the demonstration example of an EV charging in the implemented test grid. Within this section, the validation of the recognition approach is shown in the first part, while the influence of charging at different grid connection points is investigated in the second part. After the discussion of results in Section IV, the paper is concluded in Section V.

II. Load Recognition Concept and Implementation

In this section, first the general concept of load recognition is introduced. This is followed by the procedure to generate training data to enable a classifier to recognize load patterns. Then, as this study deals with the application and validation of this concept in real hardware environment, the corresponding hardware setup of this work is described. Finally, a use-case of EV detection is shown.

A. General Concept

This section describes the load recognition concept based on the grid voltage according to previous work of the authors in [18].

The goal of the proposed methodology is to recognize patterns in the voltage signal measured at a given grid connection point and to assign them to associated loads or load classes, respectively.

For this, the voltage data are acquired in time resolution of 1 s in per unit specification (pu) for a three-phase power grid. In addition, the deviation of the voltage at the current time and the voltage at one time step before are computed. Both features are combined to a multi-dimensional ($d = 2 \cdot 3$) time series S. Using a sliding window approach as applied in [29], a time series classification algorithm receives windows $w \in S^n$ as an input, which consist of a specified number n of historical data points, and returns a binary output vector $v \in \mathbb{B}^c$ every second. The length c of this vector depends on the number of trained classes, while the particular entries v_i represent the state of loads ($v_i = 1$ if a load belonging to class i is active, $v_i = 0$ if not). Thus, the recognition task is conceptualized as a multi-label

time series classification setting based on pattern recognition, mathematically expressed as

$$f : S^n \rightarrow \mathbb{B}^c \text{ with } f(w) \rightarrow v. \quad (1)$$

As shown in several fields of research, e. g., [30]–[33], tasks of this type can be successfully solved by various machine learning (ML) methods. To eventually support voltage control with the gathered knowledge about the local grid environment, a clear assignment of time series patterns to specific loads is needed. Therefore, the set of possible ML methods is restricted to supervised learning approaches instead of unsupervised ones. As the idea of the methodology is to be able to increase the number of targeted load classes, which would be required for application in real power grids, the classification task could become very complex. Therefore, in this study, the choice has been made for CNNs as they are well-known for their power in pattern recognition, shown in [34]–[37]. More precisely, as this study deals with time series data, 1D-CNNs are used. In this type of CNNs, the filters of convolutional layers are only shifted in time direction, in contrast to 2D-CNNs, which are usually used in image applications.

The overall purpose of this approach is to provide information about the local grid situation for central grid operators and decentralized generation plants in order to adapt feed-in with respect to voltage control or preferences of energy management systems.

B. Training Data Generation

In order to enable a CNN to solve the classification task described in Section II-A, the CNN has to be appropriately trained. In this regard, a training dataset containing examples of voltage patterns corresponding to the activation of targeted load classes is needed. This section deals with creating an appropriate dataset with focus on the use-case shown in Section II-D.

1) Power and Voltage Profiles: Since the availability of device-specific power profiles is rather given than that of voltage profiles, it was assumed to start with power data.

As mentioned in the previous section, the recognition is based on three-phase voltage time series data. This means, if power data are available, there is the need to generate the corresponding voltage pattern.

One possibility would be to simulate the device being active in a software-based grid model. In an optimal case, the topology of the specific use-case and the location of the device in the grid is previously known, because the voltage profile simulated in a grid model highly depends on both. Unfortunately, this knowledge is not given for every use-case and it would be necessary to choose a reference grid topology. Thus, a computationally extensive grid simulation would be required using a grid model which is unlikely to behave exactly like the one used in a particular application.

To reduce this effort in training data generation, this procedure was replaced by simple systematic calculation. This also does not guarantee to return the perfect profile for every use-case, but it speeds up the generation and increases flexibility to adapt the data for additional target loads. In detail, the following steps were performed for each phase.

- The power curve was inverted by multiplying with (–1).
- The result was rescaled and shifted to an interval $[0.9, 1.0]$, which is the lower half of the voltage tolerance band in German low voltage distribution grids [7].

This led to a profile which can be interpreted as the voltage pattern corresponding to the activation of the particular device. More precisely, it would be the maximum voltage drop which would be allowed in terms of the voltage tolerance band [7].

2) Scaling and Adding Noise: As the target load classes can be active at several grid connection points of a local grid and a different grid topology can change the voltage effects, it is not sufficient to only train the basic profile in a single magnitude, especially due to a high probability of overfitting the classifier to the specific profile values. Instead, it is necessary to consider the load activation at different positions in the grid by including scaled versions of the basic profiles. For this purpose, the basic profile was equidistantly scaled to a range of $[0.9, 1.01]$. By this, a maximum allowed voltage drop of 10 % was covered as well as a small increase of voltage despite loading the grid.

Furthermore, on one hand to avoid overfitting of the classifier and on the other hand to prepare it for noise in the power grid and disturbances caused by various grid participants, the basic profile was modified by addition of normally distributed noise with zero mean and standard deviation of ca. 0.0025. For determination of the latter, a typical single-family household power profile from HTW Berlin in [47] was transformed by the same procedure as described for the basic profile in the previous paragraph, and the standard deviation of the resulting profile was used as noise standard deviation.

The added noise does not exactly match the random noise that occurs in any power grid, nor is it representative for disturbances of other loads. However, the random noise chosen forces the CNN to focus on general behavior rather than fluctuations in the voltage. This method is sufficient for recognition success in hardware environment as shown in Section III.

After creating twenty noisy profiles, each profile was scaled to the range of $[0.97, 1.01]$ five times and also twenty times to $[0.9, 1.0]$, again considering the allowed voltage drop of 10 %. This slightly shifted the training focus to smaller deviations of the nominal voltage as they were expected in the setup during the use-case of Section II-D. All resulting profile variants were appended to the training time series with intermediate time periods of 300 s representing a non-loaded test grid.

As already mentioned for the generation of the basic voltage profile, the systematic calculations of this section were used to reduce the simulation effort. Otherwise, a large number of various grid models and simulations of the active device would have been necessary to achieve that the generated training data enables the CNN to recognize the device in a specific test case.

The number of times to scale and the parameters of noise were selected to avoid overfitting of the CNN due to too less training data and could be adapted for more complex classification tasks than considered in this paper.

C. Hardware Environment

The goal is to detect the trained loads based on a voltage signal measured at a certain grid connection point. As mentioned in Section II-A, the authors have already applied the concept for this recognition in a previous study, which was based on simulated data [18]. To realize the vision of an application in real power grids, it is necessary to take the next step by transferring the concept into real hardware environment. Therefore, the recognition of a real EV's charging process inside a hardware-based test grid was investigated in this study. More details on this are included in Section II-D.

The hardware environment was designed based on a power hardware-in-the-loop (PHIL) approach already used in [28]. In detail, a part of a test grid structure was modeled in Simulink and the remaining part was built in hardware.

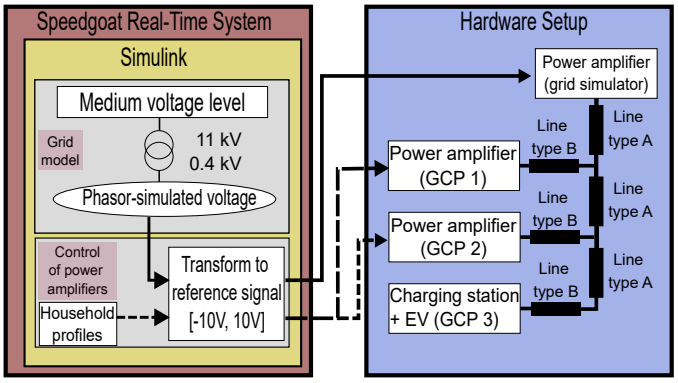

Fig. 1. Structure of the test grid implemented in real hardware using a power amplifier as a grid simulator and two different line emulator types to connect three grid connection points. These are emulated by two power amplifiers and a charging station for electric vehicles.

In the proposed test environment, shown in Fig. 1, the Simulink model contained a voltage source to include the virtual 11 kV-medium voltage level and a transformer to scale down the voltage to 400 V. In this PHIL setup, the Simulink model was executed on a Speedgoat real-time system with step-size of 150 μs.

The corresponding hardware-side of this setup was conceptualized based on reference grid no. 3 from the project MONA 2030, in which several reference grid structures were developed [38]. This low voltage grid topology was slightly reduced by removing one grid connection point. The test grid was built up in the DLR NESTEC by using the line emulator types listed in TABLE I [39].

In the test grid displayed in Fig. 1, to realize the simulated grid voltage in hardware, a 50 kVA-power amplifier from Regatron AG was used as a grid simulator to represent the upper voltage level and the power interface [40]. For this, the grid voltage, which was simulated in phasor domain, was converted into a sine wave signal. This sinusoidal signal was used to calculate a reference signal for the amplifier.

Next to this, another two 30 kVA-power amplifiers of the same manufacturer were connected at two grid connection points. By transforming a power profile into a current sine wave within the Simulink model and sending it to the hardware components via field-programmable gateway arrays (FPGA),

TABLE I
LINE EMULATOR SPECIFICATION

Name of line emulator	Parameters		
	Capacitance per unit length [nF/km]	Resistance per unit length [mΩ/km]	Inductance per unit length [μH/km]
A	15.5	6.25	31
B	9.4	26.2	24

	Equivalent line type
A	NAYY 4 × 240 mm^2, 50 m
B	NAYY 4 × 35 mm^2, 50 m

the power amplifiers can be externally controlled to represent load profiles from households for example. In addition, at the third grid connection point a charging station (type EBG compleo CITO BM2 500 2.0) was placed to enable the integration of a charging EV in the test grid [41].

The arrangement of the amplifiers and the charging station was changed in the course of this study, as described in Section II-D2.

Furthermore, a Dewesoft measurement system was used to monitor the voltage at the grid simulator's node, at the charging station and also at the grid connection points of both load emulators, while the current (and based on this the power) was only measured at the grid simulator and the charging point [42].

Following the approach presented in [28], it was not further necessary to question integrated models of certain components or their realistic interactions. Instead, real devices were used to emulate a real low voltage grid in smaller scale. By this, aspects like power grid typical noise or measurement inaccuracies from Dewesoft system were directly integrated.

D. Use-Case Electric Vehicle Detection

For validation of the proposed methodology, a demonstration example was conducted in which a CNN recognizes the charging process of an VW e-Golf inside the implemented test grid.

As a first step, a basic power profile was needed. This was obtained by a first charging test in the test grid. Thereby, the simulation model was started and the hardware components were turned on, but no external control was included to emulate real household electricity demand. This led to a three-phase power profile displayed in Fig. 2.

The Fig. 2 shows that the concerned charging process took about 50 min. During this period, the EV was AC-charged with 5 to 6 kW total power. It is noticeable here that the phases 1 and 2 were loaded, while phase 3 remained unused. In general, the power curves 1 and 2 are rectangular shaped in the large view. Nevertheless, by examining the zoom in Fig. 2, it can be observed that the EV's charging behavior showed a certain pattern consisting of a rising ramp followed by a drop.

1) Training: The obtained basic power profile was processed using the steps from Section II-B.

The resulting data profiles were concatenated to create a combined multi-dimensional time series. Then, the voltage

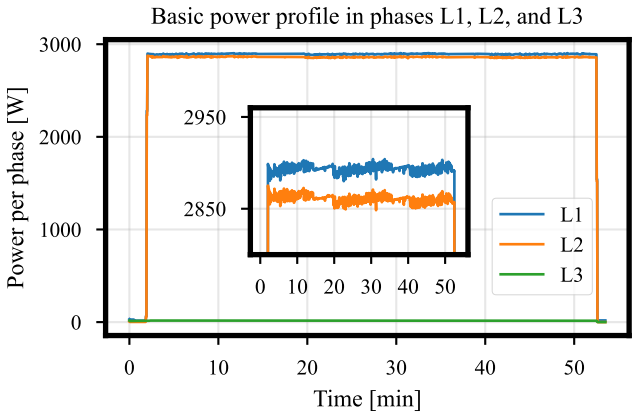

Fig. 2. Power profile of an electric vehicle charging in a non-loaded test environment for three phases. The vehicle exhibits a relatively constant profile, using only the first two phases for charging.

values were min-max-scaled using a minimum of 0.9 and a maximum of 1.0 and the difference feature values were min-max-scaled using a minimum of -0.003 and a maximum of 0.003 as in previous work [18].

After following a sliding window approach as used in [29] to prepare an input dataset for supervised learning, the CNN was trained with the AdaGrad optimization algorithm from [43]. The optimizer choice was investigated within a hyperparameter optimization in [18], considering AdaGrad, Adam, and AdaDelta algorithm [44], [45]. The respective trials were compared by a score representing the total accuracy over three different test scenarios, which means that the optimal score was 3.0. Here, several trials with AdaGrad and AdaDelta achieved scores above 2.9, with the best configuration based on AdaGrad. Next to this, Adam-based trials remained below a score of 2.0 [18]. For future work, this choice might be further investigated.

The implementation of the CNN as well as its training and evaluation were carried out using the Keras framework in Python [46]. In [18] and [19], two- or three-layer architectures were investigated. Since the presented use-case is a very simple classification task, only two-layer-based configurations of the CNN were considered in this paper. Deeper neural network architectures are expected to solve the classification task even more easily and could tend to overfit. For more complex applications, the depth of the CNN could be adapted.

2) Algorithm Validation: After generating a training dataset by the procedure from Section II-B based on the basic power profile (see Fig. 2) and training a CNN to recognize the particular EV in the voltage signal, the next step was to validate the training results. In this section, the procedure to record the needed validation data and the corresponding data preprocessing are described.

For validation of the training results, the algorithm was tested by measurement data recorded during real charging processes of an EV inside the hardware-based test grid shown in Fig. 1. To challenge the recognition algorithm by realistic grid conditions, the power amplifiers from the setup described in Section II-C were used to include two household profiles from single-family households [47]. More precisely, two profiles from 26.01.2010 were selected. Here, it was assumed that the EV starts charging around 6 pm, which followed the idea of charging after a working day. For suitable representation of a realistic grid behavior, the idea was to include representative load fluctuations as they are one of the main factors in load recognition. To quantify the fluctuations of all representative household profiles of the dataset in [47], the average standard deviation s was determined as ca. 340.35 W. After that, two sections of two profiles in the mentioned time period were selected such that their combined average standard deviation was close to s.

To generate validation data, the hardware components were turned on, the Simulink model controlling the whole setup was started, and the charging process was initiated.

This procedure was repeated three times within a slightly modified test grid. In detail, the charging station was connected to each grid connection point once, while the remaining two grid connection points were used to integrate household profiles. In these measurements, the EV showed different states of charge as listed in TABLE II.

TABLE II
MEASUREMENT SCENARIOS FOR VALIDATION/TEST DATA
CP: CHARGING POINT; H1, H2: HOUSEHOLDS NO. 1, 2

Grid connection point	Scenario number			State of charge of electric vehicle
	1	2	3	
1	CP	H1	H1	ca. 75 %
2	H1	CP	H2	ca. 50 %
3	H2	H2	CP	ca. 40 %

The voltage curves obtained at the grid connection point of the respective charging station are shown in the Fig. 3.

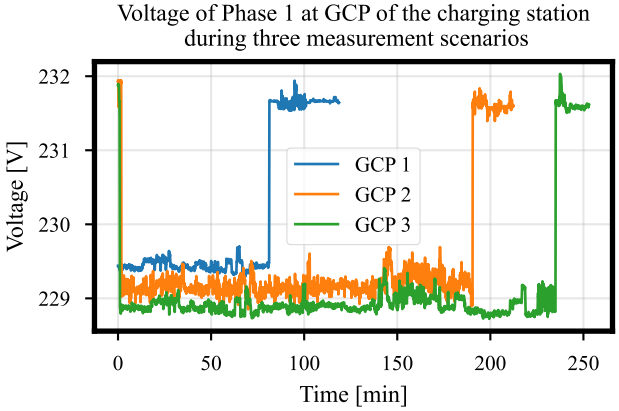

Fig. 3. Voltage curves of phase 1 measured at the grid connection point (GCP) of the charging station during three different charging scenarios. The change in the voltage level caused by the charging process increases with longer distance to the transformer of the test grid.

As Fig. 3 indicates, the different states of charge of the EV had no impact to the general shape of the associated power profile. It was also observable that the change in grid voltage during the active period increased with increasing distance between charging point and transformer.

Since the change in voltage was largest at the farthest grid connection point from the transformer, i. e., grid connection point 3, the measurement data from this position in the test grid were considered for validation. This means, the validation data were based on charging tests at three different grid connection points. For the first two scenarios, the second household profile was emulated directly at the measurement point no. 3, while the last scenario implied charging at that point.

During the charging tests, the measurement device provided phase-to-ground voltage data as rms-values for all scenarios, i. e., values around a nominal value of 230 V would be expected in real low voltage distribution grids. Due to the particular implementation of the test grid and the included components, this value was not met (see Fig. 3). Instead, by computation of the mean of all three phases during the non-loaded time period of the first measurement mentioned in the beginning of Section II-D, data were collected showing a mean value of ca. 231.43 V.

For transformation to per unit specification, all three measurement datasets created for validation were scaled to this deviating value. To create the final validation data, those three measurement datasets were concatenated to obtain a combined time series.

The analogously acquired measurement data from the other grid connection points were prepared the same way for later tests presented in Section III-B.

In validation phase, a trained CNN was required to classify time series windows from that validation dataset including a preprocessing step as described for training data. The raw output values of the CNN, which lie in an interval of $[0, 1]$, were rounded and compared to the true activity state of the EV. The performance of the CNN was evaluated based on the recognition rate, which is computed as the share of correctly classified input samples.

3) Hyperparameter Optimization: As mentioned in Section II-D1, the CNN architecture was restricted to just two convolutional layers due to the simple demonstration example for the classification. The output of both layers was calculated by using *Rectifier Linear Unit* activation functions. After the first convolutional layer, a *MaxPooling* layer reduced the data dimensionality, while the second was followed by a *GlobalAveragePooling* layer. The end of the CNN was given by a fully-connected (*Dense*) layer to compute the final classification output based on a *Sigmoid* activation function [46].

In addition, there are several untrainable parameters to define the classification task and to configure and train a CNN in order to solve the task. These so-called hyperparameters can have a large influence to the recognition performance of the CNN. Thus, similarly to previous work, a hyperparameter optimization was performed [18]. In this process, the hyperparameters listed in TABLE III were optimized using the Optuna framework (version 2.4.0) [48].

The window length defined the number of historical, multi-dimensional data points which were given into the CNN as a single sample. During the training process, the batch size was chosen to determine the number of samples considered for a single update step of the CNN's weights, while the log-normally distributed learning rate represented the step-size of these updates. Next to this, the convolutional layers of the CNN were configured by setting the number of filters and their dimension (kernel size). Thereby, the optimizer was required to set a number of filters smaller than the window length and to use a smaller kernel size in the second convolutional layer in order to increase the resolution of data examination.

TABLE III
DETAILS ON HYPERPARAMETER OPTIMIZATION AND BEST VALUES

Hyperparameter	**Possible range**	**Type, step-size**	**Best configuration**
Window length	$[50, 200]$	integer, 50	150
Batch size	$[32, 128]$	integer, 32	128
Learning rate	$[0.02, 0.05]$	log-normal, -	≈ 0.032
Filters	$[32, 96]$	integer, 32	$\{32, 32\}$
Kernel sizes	$[5, 15]$	integer, 2	$\{9, 7\}$

The hyperparameter optimizer tried several configurations of the classification with the same seed for random number generation to give every CNN the same starting position in terms of network initialization. Then, the optimizer evaluated each configuration using a particular objective function. Within this study, the respective objective value was defined as the recognition rate obtained from validation of the respective CNN.

III. RESULTS

In this section, the hyperparameter optimization results are discussed as well as the validation results of the best-configured CNN. After that, the CNN's performance at different grid connection points inside the proposed test grid (see Fig. 1) is investigated.

A. Validation Results

After the training data generation using the procedure of Section II-B. and collection of validation data as described in Section II-D2, the hyperparameter optimization presented in Section II-D3 was carried out with 50 trials.

In optimization, particularly noticeable was that larger window length tended to lead to higher recognition rates, even if the best configuration included 150 s as the window length instead of the maximum possible length of 200 s. This was a contrast to the simulative result of [19] and underlined that the recognition task in hardware environment is more complex and a larger collection of historical data points improves the recognition. However, in total, there was a variety of different parameter combinations which led to very high recognition rates, i. e., rates higher than 99 %. The best set of parameters is listed in the last column of TABLE III. This particular configuration yielded the results shown in Fig. 4.

In Fig. 4, the upper graph shows the comparison of the CNN's raw output (blue) from classifying the validation time series and the true activity state of the EV (orange). The corresponding three-phase voltage time series is displayed in the bottom graph. It can be noticed that the CNN's output was very close to the true values, especially during the off-periods of the EV. Another observation in the bottom graph

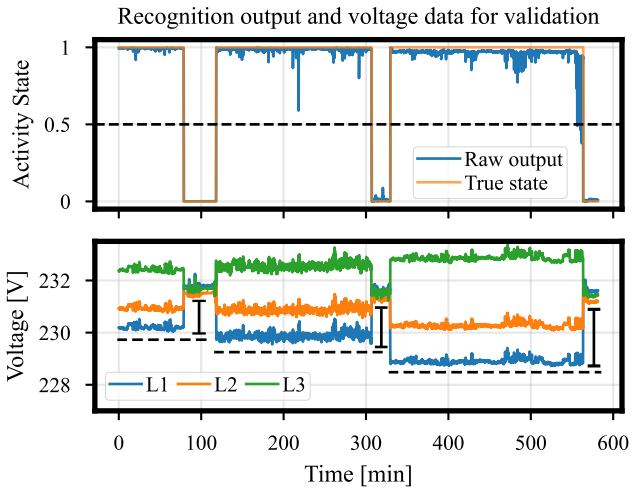

Fig. 4. Raw recognition output of the convolutional neural network during validation approximating the true output and the related voltage time series.

is that the change in voltage at the third grid connection point during the EV's active period increased with increasing distance of the charging point to the transformer. This is illustrated by the black distance markers that increase in length. That relation apparently led to more fluctuation in the raw output. Thus, there were larger deviations between raw output and true state. Additionally, it can be suspected that the integrated household profiles worsen the recognition. For example, around a time point of ca. 470 min, the fluctuation in the voltage curves increased due to influences of the household profiles. At the same time, the deviation of the raw output curve to the true state increased. However, after rounding the raw output, the recognition results were nearly perfect, and thus the recognition rate was very close to 100 %, as shown in Fig. 5.

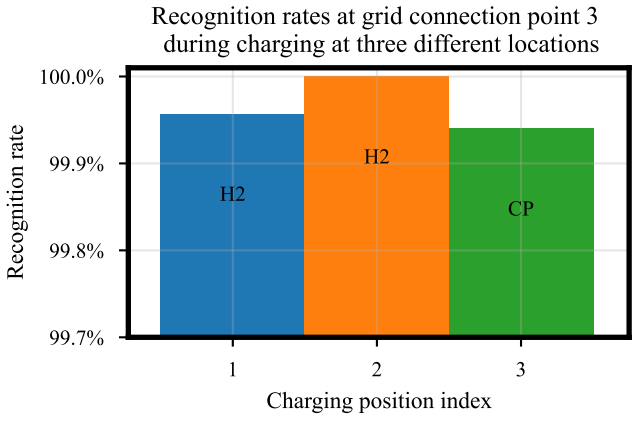

Fig. 5. Nearly perfect recognition rates based on voltage measurement at grid connection point (GCP) no. 3 in case of charging at three different grid locations. While charging was performed at position 1 and 2 (CP), the household profile (H2) was emulated at GCP no. 3.

In Fig. 5, the bar plot shows the recognition rates obtained during validation phase, which was based on measurement data from grid connection point 3 in the test grid (see Fig. 1) during three different charging scenarios implying to charge the EV at different grid connection points. Each bar of the plot represents the rate for a single scenario.

It can be seen that the recognition rates for all three scenarios were higher than 99.9 %. Since the validation data showed an imbalance of 13.8 % off-period of the EV to 86.2 % active time, these values were further investigated. More precisely, F1 score (harmonic mean of precision and recall) and balanced accuracy (mean of true positive and the true negative rate) were computed. The resulting values were also higher than 99.9 %. This means that the classifier performs accurately during both active and inactive times of the EV. In total, this is nearly perfect performance. However, it has to be considered that the use-case represented a very simple demonstration example. This is discussed in more detail in the following section, in which the performance of this CNN is further investigated.

B. Comparison of Charging at Different Grid Positions

From the promising results of the previous section, the next step was to test the CNN by the complete measurement data from the charging tests. This means, the CNN was required to classify the measurement data acquired in all three scenarios listed in TABLE II with measurements at all grid connection points of the test grid. In other words, each cell of that table yielded a single test dataset.

Similar to the validation results, the bars in Fig. 6 show the recognition rates on those test datasets.

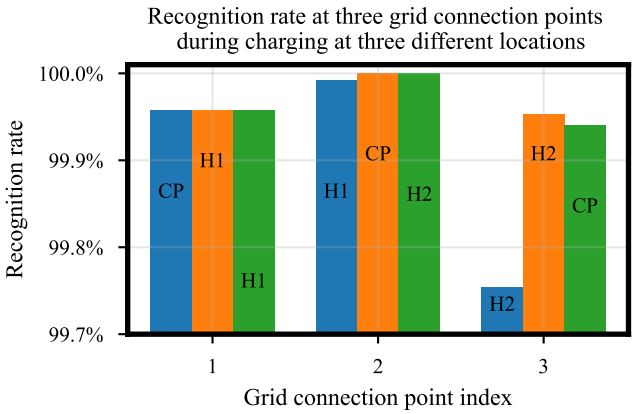

Fig. 6. Bar plot of recognition rates for the cases of grid voltage measurement at each grid connection point (GCP) of the test grid while charging at different GCPs; blue: rate for charging at GCP no. 1, orange: rate for charging at GCP no. 2, green: rate for charging at GCP no. 3.

As for the validation, all recognition rates were higher than 99.7 %, which was similarly achieved using the F1 score and balanced accuracy on these test data. The Fig. 6 shows that there are some differences between the rates observable, but they are very small. It can be suspected that they are caused by numeric reasons or the different compositions of active and inactive times of the EV in the test datasets. Another factor could be the slightly different temporal overlay of the household profiles and the charging process. Moreover, the

different positioning of the charging station affected the grid voltage behavior, and therefore, the recognition performance was slightly changed. That effect could be increased under different composition of loads in the test grid with higher power demands.

IV. Discussion

As mentioned in the previous section, the high recognition rates from Fig. 5 and Fig. 6 were to be expected due to simplicity of the use-case. The demonstration example is considered as simple for several reasons. First, there was only one load to be detected by the CNN. Second, the power demand of the EV was significantly higher than the demand of the households. The third reason is the special behavior of the EV during charging process. Since the charging of this particular EV caused the voltage to drop at two phases and to raise at the third, the load pattern was quite special and easy to detect. In this regard, it has to be remarked that there are some EVs, which are designed to charge on three phases as well as others which utilize two or just a single phase. Hence, the use-case is simple but it involves a typical and real occurring load. An EV that uses all three phases for charging could be harder to detect because it might be more complicated to distinguish its voltage effects from voltage changes caused by other devices.

To further analyze the proposed concept, it would be conceivable to create more complex classification scenarios in very different ways. For example, more household profiles could be integrated, e. g., with stronger deviations. It would also be interesting how to deal with more charging EVs in the test grid. Their single profiles would be trained as well as overlapping profiles, as already examined in [18] within simulation environment. The resulting increase in grid voltage fluctuations would strongly raise the level of difficulty, especially in hardware environment. Additionally, further load classes like heat pumps could be integrated in the test grid. For such scenarios, especially in applications in real power grids, it might be necessary to adapt the generation of training data. In particular, it could be investigated how noise, which currently comes from simple normal distribution, can be generated more appropriately to disturbances of other active devices with a strong influence on the grid voltage.

In this study, it was found that most of the hyperparameters mentioned for task configuration did not have a major impact on the performance. This can be explained by the simplicity of the use-case. It is expected that this would change with increasing complexity of the classification setting. In addition, it would be of interest to examine the number of convolutional layers and the choice of the optimizer as well as topics like initialization of the neural network's weights.

In general, this paper dealt with a simple use-case of an EV detection in hardware environment. This led to promising results, but their robustness needs to be analyzed in more complex grid situations.

However, in developing new approaches, especially for voltage control or supporting strategies like load recognition, respectively, simple use-cases are preferable to advance development.

For this, the proposed work presents an environment consisting of real hardware components, which allows to validate a recognition algorithm in a safe and controllable area.

The presented use-case illustrated the general capability of recognizing loads even in real hardware environment using the proposed concept. In addition, this use-case emphasized the advantage to collect the voltage of all three grid phases. With the concept investigated in this study, on one hand it is possible to recognize historical pattern of trained loads in the voltage signal, and on the other hand, the algorithm is able to examine the relation of the phases without expensively calculating phase angles.

Finally, the classification algorithm was able to recognize the charging process of a real EV in the implemented hardware-based test grid under disturbance of two household profiles for almost all test data points.

V. Conclusion

The proposed study presented a concept for load recognition in low voltage distribution grids based on the voltage measured at a single grid connection point. This concept was applied within a test grid structure built in real hardware to detect an EV charging in the grid.

The test environment was implemented based on a reference grid topology and included a real charging station as well as two power amplifiers to emulate two grid nodes with two household power profiles.

After starting with a basic power profile of the particular EV, a systematic methodology was followed based on simple calculations and addition of noise to create a combined time series. With this data and a sliding window approach, a CNN was trained to recognize the particular EV despite disturbances like hardware effects and further active grid participants.

To validate and test the CNN, several charging tests were conducted in order to collect measurement data from three scenarios. This test series contained charging at all three grid connection points of the test grid. During the charging tests, data from all grid connection points were acquired and preprocessed. After that, the trained CNN was required to classify the measurement data. The classification results were very accurate as the CNN achieved recognition rates of above 99.7 % for all test datasets. In order to properly interpret this highly accurate performance, it has to be mentioned that the use-case was quite simple, especially because of an asymmetric charging behavior of the EV. Nevertheless, this demonstration example showed that a CNN, which was trained following a systematic training data generation method, can be enabled to recognize loads in a real hardware environment, which includes real hardware influences, noisy voltage measurements, and overlapping voltage profiles of other devices.

Future work on this topic will investigate the associated limits of the load recognition concept, especially within more complex grid situations involving more active grid participants, which might show more complex power profiles. The extension of the concept to aim for more than one load type would also be interesting because it would require the CNN to examine the voltage signal for more than a single pattern.

By this, the CNN's power in pattern recognition within this application would be investigated to a further extent. Next to this, the influences of larger grid topologies implemented in hardware could be examined. Especially interesting would be the application of the method to real-world distribution grids. These possible studies could require to adapt the overall methodology in terms of training data generation and configuration of the CNN. However, further investigations could deal with the integration of this concept into voltage control.

In summary, it can be stated that the proposed study showed a successful approach to detect an active load inside a real low voltage grid despite challenges like hardware effects and power grid typical noise, measurement inaccuracies, and other disturbing grid participants. Thus, these promising results show that the presented methodology can support future strategies for voltage control by provision of information about the current grid situation.

ACKNOWLEDGMENTS

Thanks to Vanessa Beutel, Thomas Esch, and Holger Behrends for their support in implementation of the hardware-based test grid and carrying out the charging tests. The authors also would like to thank Ode Bokker and Moiz Ahmed for their advice in grid simulations and use of the real-time system.

REFERENCES

[1] Arbeitsgruppe Erneuerbare Energien – Statistik, "Erneuerbare Energien 2020," Bundesministerium für Wirtschaft und Energie (BMWi), Berlin, Tech. Rep., Mar. 2021. [Online]. Available: https://www.erneuerbare-energien.de/EE/Redaktion/DE/Downloads/Berichte/erneuerbare-energien-2020.pdf

[2] Federal Ministry for the Environment, Nature Conservation, and Nuclear Safety (BMU), "Climate Action Programme 2030: Measures to achieve the 2030 climate protection goals, Berlin, Tech. Rep., Oct. 2019.

[3] Deutsche Energie-Agentur GmbH, Technische Universität Dortmund, ef.Ruhr GmbH, "dena-Studie Systemdienstleistungen 2030," Deutsche Energie-Agentur GmbH, Berlin, Tech. Rep., Feb. 2014.

[4] K.-H. Backhaus, D. H. Ehrhardt, A. Jacob, L. Petereit, D. B. Schreinermacher, A. Sperr, E. Tippelt, and V. Weinmann, "Branchenstudie 2021: Marktanalyse – Szenarien – Handlungsempfehlungen," Bundesverband Wärmepumpe (BWP) e. V., Berlin, Tech. Rep., Jul. 2021.

[5] A. Tavakoli, S. Saha, M. T. Arif, M. E. Haque, N. Mendis, and A. M. Oo, "Impacts of grid integration of solar PV and electric vehicle on grid stability, power quality and energy economics: a review," *IET Energy Systems Integration*, vol. 2, no. 3, pp. 243–260, Sep. 2020. [Online]. Available: https://digital-library.theiet.org/content/journals/10.1049/iet-esi.2019.0047

[6] C. H. Dharmakeerthi, N. Mithulananthan, and T. K. Saha, "Impact of electric vehicle fast charging on power system voltage stability," *International Journal of Electrical Power & Energy Systems*, vol. 57, pp. 241–249, May 2014. [Online]. Available: https://www.sciencedirect.com/science/article/pii/S0142061513005218

[7] Deutsche Kommission für Elektrotechnik, Elektronik und Informationstechnik im DIN und VDE, "DIN EN 50160: Merkmale der Spannung in öffentlichen Elektrizitätsversorgunsnetzwerken," Deutsches Institut für Normung e. V., Berlin, DIN-Norm, 2011.

[8] K. Beyer, R. Beckmann, S. Geißendörfer, K. von Maydell, and C. Agert, "Adaptive Online-Learning Volt-Var Control for Smart Inverters Using Deep Reinforcement Learning," *Energies*, vol. 14, no. 7, p. 1991, Jan. 2021, Publisher: Multidisciplinary Digital Publishing Institute. [Online]. Available: https://www.mdpi.com/1996-1073/14/7/1991

[9] H. Liu and W. Wu, "Online Multi-Agent Reinforcement Learning for Decentralized Inverter-Based Volt-VAR Control," *IEEE Transactions on Smart Grid*, vol. 12, no. 4, pp. 2980–2990, Jul. 2021.

[10] Q. Yang, G. Wang, A. Sadeghi, G. B. Giannakis, and J. Sun, "Two-Timescale Voltage Control in Distribution Grids Using Deep Reinforcement Learning," *IEEE Transactions on Smart Grid*, vol. 11, no. 3, pp. 2313–2323, May 2020.

[11] G. Hart, "Nonintrusive appliance load monitoring," *Proceedings of the IEEE*, vol. 80, no. 12, pp. 1870–1891, Dec. 1992.

[12] E. J. Aladesanmi and K. A. Folly, "Overview of non-intrusive load monitoring and identification techniques," *IFAC-PapersOnLine*, vol. 48, no. 30, pp. 415–420, Jan. 2015. [Online]. Available: https://www.sciencedirect.com/science/article/pii/S2405896315030566

[13] K. Brucke, S. Arens, J.-S. Telle, T. Steens, B. Hanke, K. von Maydell, and C. Agert, "A Non-Intrusive Load Monitoring Approach for Very Short Term Power Predictions in Commercial Buildings," *arXiv:2007.11819 [eess, stat]*, Jul. 2020. [Online]. Available: http://arxiv.org/abs/2007.11819

[14] L. de Diego-Otón, D. Fuentes-Jimenez, A. Hernández, and R. Nieto, "Recurrent LSTM Architecture for Appliance Identification in Non-Intrusive Load Monitoring," in *2021 IEEE International Instrumentation and Measurement Technology Conference (I2MTC)*, May 2021, pp. 1–6, iSSN: 2642-2077.

[15] T. Bernard, "Non-Intrusive Load Monitoring (NILM): combining multiple distinct electrical features and unsupervised machine learning techniques," Jul. 2018. [Online]. Available: https://d-nb.info/1163534102/34

[16] A. A. Munshi and Y. A.-R. I. Mohamed, "Unsupervised Nonintrusive Extraction of Electrical Vehicle Charging Load Patterns," *IEEE Transactions on Industrial Informatics*, vol. 15, no. 1, pp. 266–279, Jan. 2019.

[17] K. Basu, V. Debusschere, S. Bacha, U. Maulik, and S. Bondyopadhyay, "Nonintrusive Load Monitoring: A Temporal Multilabel Classification Approach," *IEEE Transactions on Industrial Informatics*, vol. 11, no. 1, pp. 262–270, Feb. 2015.

[18] H. Schlachter, S. Geißendörfer, K. von Maydell, and C. Agert, "Voltage-Based Load Recognition in Low Voltage Distribution Grids with Deep Learning," *Energies*, vol. 15, no. 1, p. 104, Jan. 2022, Publisher: Multidisciplinary Digital Publishing Institute. [Online]. Available: https://www.mdpi.com/1996-1073/15/1/104

[19] H. Schlachter, S. Geißendörfer, K. von Maydell, and C. Agert, "Voltage-Based Heat Pump Recognition with Convolutional Neural Networks," in *2022 IEEE PES Conference on Innovative Smart Grid Technologies Europe (ISGT)*, Oct. 2022.

[20] M. Thornton, M. Motalleb, H. Smidt, J. Branigan, P. Siano, and R. Ghorbani, "Internet-of-Things Hardware-in-the-Loop Simulation Architecture for Providing Frequency Regulation With Demand Response," *IEEE Transactions on Industrial Informatics*, vol. 14, no. 11, pp. 5020–5028, Nov. 2018.

[21] M. E.-S. M. Essa, J. V. W. Lotfy, and M. E. K. Abd-Elwahed, "Adaptive Neural Network Predictive Control Design for Hybrid Electric Vehicle with Hardware in the Loop (HIL) Verification," in *2021 17th International Computer Engineering Conference (ICENCO)*, Dec. 2021, pp. 118–123, iSSN: 2475-2320.

[22] R. Han, R. Lian, H. He, and X. Han, "Continuous Reinforcement Learning Based Energy Management Strategy for Hybrid Electric Tracked Vehicles," *IEEE Journal of Emerging and Selected Topics in Power Electronics*, pp. 1–1, 2021.

[23] C. González-Castaño, J. Marulanda, C. Restrepo, S. Kouro, A. Alzate, and J. Rodriguez, "Hardware-in-the-Loop to Test an MPPT Technique of Solar Photovoltaic System: A Support Vector Machine Approach," *Sustainability*, vol. 13, no. 6, p. 3000, Jan. 2021, Publisher: Multidisciplinary Digital Publishing Institute. [Online]. Available: https://www.mdpi.com/2071-1050/13/6/3000

[24] L. De Herdt, A. Shekhar, Y. Yu, G. R. C. Mouli, J. Dong, and P. Bauer, "Power Hardware-in-the-Loop Demonstrator for Electric Vehicle Charging in Distribution Grids," in *2021 IEEE Transportation Electrification Conference & Expo (ITEC)*, Jun. 2021, pp. 679–683, iSSN: 2377-5483.

[25] A. Hoke, S. Chakraborty, and T. Basso, "A power hardware-in-the-loop framework for advanced grid-interactive inverter testing," in *2015 IEEE Power & Energy Society Innovative Smart Grid Technologies Conference (ISGT)*, Feb. 2015, pp. 1–5.

[26] M. Muhammad, H. Behrends, S. Geißendörfer, K. v. Maydell, and C. Agert, "Power Hardware-in-the-Loop: Response of Power Components in Real-Time Grid Simulation Environment," *Energies*, vol. 14, no. 3, p. 593, Jan. 2021, Publisher: Multidisciplinary Digital Publishing Institute. [Online]. Available: https://www.mdpi.com/1996-1073/14/3/593

[27] F. Ebe, B. Idlbi, D. E. Stakic, S. Chen, C. Kondzialka, M. Casel, G. Heilscher, C. Seitl, R. Bründlinger, and T. I. Strasser, "Comparison of Power Hardware-in-the-Loop Approaches for the Testing of Smart

Grid Controls," *Energies*, vol. 11, no. 12, p. 3381, Dec. 2018, Publisher: Multidisciplinary Digital Publishing Institute. [Online]. Available: https://www.mdpi.com/1996-1073/11/12/3381

[28] M. Ahmed, H. Schlachter, V. Beutel, T. Esch, S. Geißendörfer, and K. von Maydell, "Grid-in-the-Loop Environment for Stability Investigations of Converter-Dominated Distribution Grids," in *2022 IEEE 13th International Symposium on Power Electronics for Distributed Generation Systems*, 2022.

[29] O. Krystalakos, C. Nalmpantis, and D. Vrakas, "Sliding Window Approach for Online Energy Disaggregation Using Artificial Neural Networks," in *Proceedings of the 10th Hellenic Conference on Artificial Intelligence*. Patras Greece: ACM, Jul. 2018, pp. 1–6. [Online]. Available: https://dl.acm.org/doi/10.1145/3200947.3201011

[30] J. Wang, Y. Yang, J. Mao, Z. Huang, C. Huang, and W. Xu, "CNN-RNN: A Unified Framework for Multi-label Image Classification," in *2016 IEEE Conference on Computer Vision and Pattern Recognition (CVPR)*, Jun. 2016, pp. 2285–2294, iSSN: 1063-6919.

[31] Y. Li and Y. Wang, "A Multi-label Image Classification Algorithm Based on Attention Model," in *2018 IEEE/ACIS 17th International Conference on Computer and Information Science (ICIS)*, Jun. 2018, pp. 728–731.

[32] L. Song, J. Liu, B. Qian, M. Sun, K. Yang, M. Sun, and S. Abbas, "A Deep Multi-Modal CNN for Multi-Instance Multi-Label Image Classification," *IEEE Transactions on Image Processing*, vol. 27, no. 12, pp. 6025–6038, Dec. 2018.

[33] L. Massidda, M. Marrocu, and S. Manca, "Non-Intrusive Load Disaggregation by Convolutional Neural Network and Multilabel Classification," *Applied Sciences*, vol. 10, no. 4, p. 1454, Jan. 2020, Publisher: Multidisciplinary Digital Publishing Institute. [Online]. Available: https://www.mdpi.com/2076-3417/10/4/1454

[34] H. I. Fawaz, G. Forestier, J. Weber, L. Idoumghar, and P.-A. Muller, "Deep learning for time series classification: a review," *Data Mining and Knowledge Discovery*, vol. 33, no. 4, pp. 917–963, Jul. 2019, arXiv: 1809.04356. [Online]. Available: http://arxiv.org/abs/1809.04356

[35] Y. Qian, M. Bi, T. Tan, and K. Yu, "Very Deep Convolutional Neural Networks for Noise Robust Speech Recognition," *IEEE/ACM Transactions on Audio, Speech, and Language Processing*, vol. 24, no. 12, pp. 2263–2276, Dec. 2016.

[36] A. Krizhevsky, I. Sutskever, and G. E. Hinton, "ImageNet classification with deep convolutional neural networks," *Communications of the ACM*, vol. 60, no. 6, pp. 84–90, May 2017. [Online]. Available: https://dl.acm.org/doi/10.1145/3065386

[37] A. Ashiquzzaman and A. K. Tushar, "Handwritten Arabic numeral recognition using deep learning neural networks," in *2017 IEEE International Conference on Imaging, Vision Pattern Recognition (icIVPR)*, Feb. 2017, pp. 1–4.

[38] S. Köppl, A. Bruckmeier, F. Böing, M. Hinterstocker, B. Kleinertz, and C. Konetschny, "Projekt MONA 2030: Grundlage für die Bewertung von netzoptimierenden Maßnahmen: Teilbericht Basisdaten," Forschungsstelle für Energiewirtschaft e.V. (Ffe), München, Tech. Rep., 2017.

[39] K. von Maydell, J. Petznik, H. Behrends, T. Esch, M. Ahmed, A. Rubio, L. Uhse, R. Völker, S. Unglaube, S. Geißendörfer, F. Schuldt, and C. Agert, "The Networked Energy Systems Emulation Center at the German Aerospace Center DLR – bridging the gap between digital simulation and real operation of energy grids," *At-Automatisierungstechnik*, vol. 70, no. 12, pp. 1072–1083, 2022.

[40] Regatron AG, "TC.ACS Series - Regatron," 2022. [Online]. Available: https://www.regatron.com/service/download/#manuals

[41] EBG Compleo GmbH, "EBG Compleo CITO BM2 500 2.0," 2019. [Online]. Available: https://pub-mediabox-storage.rxweb-prd.com/exhibitor/document/e2c22e9f-8306-4880-836f-6e42a889b7ae

[42] Dewesoft Inc., "SIRIUS® | Powerful USB and EtherCAT DAQ System | Dewesoft." [Online]. Available: https://dewesoft.com/products/daq-systems/sirius

[43] J. Duchi, E. Hazan, and Y. Singer, "Adaptive Subgradient Methods for Online Learning and Stochastic Optimization," *Journal of Machine Learning Research*, vol. 12, pp. 2121–2359, 2011.

[44] D. P. Kingma and J. Ba, "Adam: A Method for Stochastic Optimization," *arXiv:1412.6980 [cs]*, Jan. 2017. [Online]. Available: http://arxiv.org/abs/1412.6980

[45] M. D. Zeiler, "ADADELTA: An Adaptive Learning Rate Method," *arXiv:1212.5701 [cs]*, Dez. 2012. [Online]. Available: http://arxiv.org/abs/1212.5701

[46] F. Chollet, "Keras," 2015. [Online]. Available: https://keras.io

[47] T. Tjaden, J. Bergner, J. Weniger, and V. Quaschning, "Repräsentative elektrische Lastprofile für Wohngebäude in Deutschland auf 1-sekündiger Datenbasis," Hochschule für Technik und Wirtschaft (HTW Berlin), Dataset, 2015.

[48] T. Akiba, S. Sano, T. Yanase, T. Ohta, and M. Koyama, "Optuna: A Next-generation Hyperparameter Optimization Framework," in *Proceedings of the 25th ACM SIGKDD International Conference on Knowledge Discovery & Data Mining*, ser. KDD '19. New York, NY, USA: Association for Computing Machinery, Jul. 2019, pp. 2623–2631. [Online]. Available: https://doi.org/10.1145/3292500.3330701

BIOGRAPHIES

Henning Schlachter studied at the Carl von Ossietzky University of Oldenburg, where he received his master's degree in Mathematics. He completed internships at the Technical University of Clausthal and at the Institute of Aerodynamics and Flow Technology, German Aerospace Center. Currently, he is employed at the German Aerospace Center, where he works in the Institute of Networked Energy Systems as a PhD student. Here, his special fields of interest are intelligent and grid-supporting converter control and machine learning applications. He has already published a journal paper and several conference contributions in the research field of the presented study.

Stefan Geißendörfer studied physics at the University of Wurzburg, Germany, and completed his diploma in 2008. In 2009 he moved to the EWE research center for energy technology 'NEXT ENERGY', a research institute at the University of Oldenburg, Germany. In Oldenburg he received his PhD degree in physics in 2013 for his research in the field of photovoltaics and continued as post-doc until 2016. During this time, he was project manager and took over the management of the research group 'Product Development & Integration'. In 2017 he worked as a consultant for semiconductor components in the automotive sector for FERCHAU Engineering GmbH in Munich, Germany, and also worked on the standardization of EV charging station infrastructure. At the end of 2017 he moved to the DLR Institute for Networked Energy Systems in Oldenburg, Germany, as a project manager and founded a new research group for power grid technologies in 2018. His research interests include the hardware development of technologies for electrical distribution grids, such as inverters and converters, and their intelligent control technology for robust grid operation with high penetration of decentralized generating units.

Karsten von Maydell received the MSc degree in physics from the University of Oldenburg, Germany in 2000 and the PhD degree in physics from the University of Marburg, Germany, in 2003. From 2000 to 2006, he worked as a graduate research assistant and postdoctoral researcher and project manager at the Helmholtz-Zentrum Berlin. From 2006 to 2007, he worked as a project manager R&D at Q-Cells AG Thalheim, Germany and from 2007 to 2008, he was group leader at the Energy and Semiconductor Research laboratory at the University of Oldenburg. He was head of division Photovoltaic from 2008 to 2014 at the NEXT ENERGY research institute in Oldenburg, Germany. Since 2017, he is the head of Energy Systems Technology department at the DLR Institute of Networked Energy Systems. His research interests include the design of energy systems, smart energy management for grid connected and off-grid connected systems, integration of flexibilities in energy systems and robust operation of power grids.

Carsten Agert studied Physics at the University of Marburg, Germany, and the University of Canterbury, UK. As a scholar of the Studienstiftung he completed his Ph.D. in Physics in 2001, based on his research work at the Fraunhofer Institute for Solar Energy Systems in Freiburg, Germany, and at the University of Oxford, UK. In 2001 he worked as a Postdoctoral Researcher in Pretoria, South Africa. From 2002 to 2005, he was a Research Associate with the German Advisory Council on Global Change WBGU. Subsequently he was the head of the Fuel Cell Systems Research Group at the Fraunhofer Institute for Solar Energy Systems, from 2005 to 2008. Since 2008, he is a full professor at the University of Oldenburg and director of the DLR Institute of Networked Energy Systems, until 2017 known as NEXT ENERGY institute. His research interests include materials and device development for energy converters, research into electrical energy technologies and systems as well as energy systems analysis.